Chemical Engineering Journal 165 (2010) 806–812

Contents lists available at ScienceDirect

Chemical Engineering Journal

journal homepage: www.elsevier.com/locate/cej

Catalytic ozonation of atrazine and linuron on MnO_x/Al_2O_3 and MnO_x/SBA-15 in a fixed bed reactor

Roberto Rosal*, María S. Gonzalo, Antonio Rodríguez, José Antonio Perdigón-Melón, Eloy García-Calvo

Departamento de Química Analítica e Ingeniería Química, Universidad de Alcalá, E-28771 Alcalá de Henares, Spain

ARTICLE INFO

Article history:
Received 8 July 2010
Received in revised form 4 October 2010
Accepted 9 October 2010

Keywords:
Heterogeneous catalytic ozonation
Fixed bed
Manganese oxide
SBA-15 supported catalyst
Hydroxyl radicals

ABSTRACT

The catalytic ozonation of the herbicides atrazine and linuron was studied in a fixed-bed reactor using alumina-supported manganese oxide catalysts. Two manganese oxides were supported, one on activated alumina, MnO_x/Al_2O_3, the other, MnO_x/SBA-15, after impregnating mesoporous silica by the minimum volume method. The adsorption of both compounds was not significant and the kinetic data indicated that the reaction with molecular ozone was a non-catalytic process which took place in homogeneous phase. The results of catalytic runs also showed no evidence that any of the catalysts increased the rate of the hydroxyl-mediated ozonation. Both catalysts, however, considerably increased the ozone decomposition rate constant, particularly MnO_x/SBA-15 for which a MnO_x bed load of 1.0 wt.% as MnO_2 resulted in a 30 fold increase with respect to the homogeneous rate. The catalysts also improved the efficiency in the production of hydroxyl radicals from ozone with an average hydroxyl radical-to-ozone ratio as high as 10^{-6} for MnO_x/Al_2O_3 and 3.0×10^{-6} for MnO_x/SBA-15. The catalysts also led to lower ozone consumption per mole of converted organic compound, whether or not bicarbonate was present in the solution. Best results were obtained in all cases for MnO_x/SBA-15, most probably due to a better distribution of the active phase on a larger surface.

1. Introduction

There is a growing need for treatment technologies that can provide safe treated effluents from wastewater treatment plants (WWTP) in order to enhance wastewater reuse. Organic compounds, particularly those belonging to emerging groups such as pharmaceuticals and personal care products, severely endanger water reuse in many applications even if they are present in very low amounts. Besides affecting reuse strategies, micropollutants from WWTP are currently discharged to surface bodies, thus jeopardising the environmental protection of water bodies. In this regard, Member States of the European Union have been urged to introduce policies under the EC Water Framework Directive with a view to achieving good ecological water status in terms of the presence of chemicals from human activity in a period covering fifteen years from 2015, the date this Directive comes into force [1].

The available technologies for the removal of micropollutants include many oxidation processes carried out alone or in combination with membrane separations. A wide variety of oxidation processes have been proposed for the removal of organic compounds from WWTP, most of them belonging to the category of advanced oxidation processes (AOP). AOP are those oxidation processes based on the generation of highly reactive species, particularly hydroxyl radicals, whose use has been proposed for the degradation of many classes of organic compounds, especially when their chemical stability makes them difficult to degrade otherwise [2]. AOP is a growing family of technologies that differ in the way they generate the primary oxidant species, the hydroxyl radical. They include a number of combined processes in which the simultaneous use of several technologies aims at increased economic efficiency or better suitability to certain streams [3,4].

Among them, considerable research effort has recently been centred on investigating heterogeneous catalytic ozonation. In this process, a solid catalyst may (i) adsorb and decompose ozone, thereby leading to the formation of active species which then react with non-chemisorbed organics; and (ii) adsorb organic molecules with further reaction with oxidants either adsorbed and surface-generated or from the bulk [5]. Apart from these general ideas, the exact mechanism of catalytic ozonation is still not clear. In metals or metal oxides, the catalytic reaction might involve the adsorption of organic molecules or ions with subsequent oxidation by Eley–Rideal or Langmuir–Hinshelwood interaction with oxidant species. It is well known that the adsorption of neutral compounds on oxides in aqueous solutions has to overcome the competitive adsorption of water molecules and that adsorption is relatively favoured for ionizable compounds if the surface is charged [5].

* Corresponding author. Tel.: +34 918855099; fax: +34 918855088.
E-mail address: roberto.rosal@uah.es (R. Rosal).

1385-8947/$ – see front matter © 2010 Elsevier B.V. All rights reserved.
doi:10.1016/j.cej.2010.10.020

Nomenclature

r_A	rate of ozonation of a given compound, mol L^{-1} s^{-1} or mol kg^{-1} s^{-1}
r_{O_3}	rate of reaction of ozone, mol L^{-1} s^{-1} or mol kg^{-1} s^{-1}
k_{O_3}	second order rate constant for direct ozonation reaction, L mol^{-1} s^{-1} (homogeneous) or L^2 mol^{-1} kg^{-1} s^{-1} (catalytic)
k_{ox}	second order rate constant of surface reaction, L mol^{-1} s^{-1}
k_d	rate constant for the decomposition of ozone, s^{-1} (homogeneous) or L kg^{-1} s^{-1} (catalytic)
$k_{HO\bullet}$	second order rate constant for the reaction with hydroxyl radicals, L mol^{-1} s^{-1}
c_A, c_B	concentration of organic compounds, mol L^{-1}
$c_{HO\bullet}$	concentration of hydroxyl radical, mol L^{-1}
c_{O_3}	concentration of dissolved ozone, mol L^{-1}
$c_{(O_3)_s}$	concentration of adsorbed ozone, mol kg^{-1}
c_s	concentration of free active centres at the catalyst surface, mol kg^{-1}
c_{ox}	concentration of oxidized surface sites, mol kg^{-1}
c_t	total concentration of active sites, mol kg^{-1}
K	equilibrium constant of ozone adsorption, L mol^{-1}
R_{ct}	ratio of $c_{HO\bullet}$ to c_{O_3}, dimensionless
R^c	ratio of $c_{(O_3)_s}$ and c_{O_3}, L kg^{-1}
W	mass of catalyst, kg
F_o	liquid flow-rate in reactor feed, L s^{-1}

Greek symbols

ν	stoichiometric coefficient, dimensionless
ε	bed porosity, dimensionless
ρ_b	bed bulk density, g L^{-1}

Subscripts and superscripts

o	reactor inlet
s	reactor outlet
h	homogeneous reaction
c	catalytic reaction
hc	simultaneous homogeneous and catalytic reaction

Although it is generally true that the extent of adsorption considerably decreases under the unfavourable electrostatic conditions that take place on charged surfaces, it has been pointed out that small but significant adsorption may occur even in this case through surface complexation reactions [6]. In a previous paper, we determined that the use of Al_2O_3 or MnO_x/Al_2O_3 catalysts did not result in an increase in the indirect ozonation rate constant of fenofibric acid with respect to homogeneous ozonation, a fact that suggests the absence of surface interaction with fenofibric acid, a compound completely dissociated in working conditions [7].

The use of three-phase beds for heterogeneous catalytic ozonation was originally developed as part of the Ecoclear process, and originally intended for the use of granular activated carbon (GAC) to remove chlorinated hydrocarbons in contaminated groundwater [8]. From then on, most applications of catalytic ozonation which used fixed or fluidized beds were linked to GAC or metal/metal oxides supported on GAC. [9,10]. Recently, there have been reports of the use of activated carbon fibers for the ozonation of phenol in an aqueous fluidized bed reactor in which a significant reduction of the isoelectric point (IEP) of the surface took place as a consequence of the production of surface oxygen-containing groups [11]. Contrary to agitated reactors, that exhibit a high liquid-to-catalyst ratio, fixed-bed reactors can limit parallel homogeneous reactions such as polymerisation or the formation of other by-products. In this work, we studied the ozonation of the herbicides atrazine and linuron, two non-polar pollutants commonly encountered in wastewater from agricultural activities. The complexity of gas–liquid–solid reactions is a well-known factor that complicates the use of reactors operating in packed-bubble or trickle-bed modes. Accordingly, in this work we used a two-phase heterogeneous catalytic reactor operating with an ozone-preloaded aqueous buffer that facilitated our goal of studying the efficiency of production of hydroxyl radicals of two manganese-based catalysts using a low-liquid-to-catalyst ratio. For this purpose we compared a classic manganese oxide supported on activated alumina with a MnO_x/SBA-15 catalyst.

In spite of the considerable research in the field of catalytic ozonation performed during last years, the mechanism of catalytic processes is still essentially unknown. It has been demonstrated that several catalysts enhance the efficiency of ozonation but the mechanism of this process, particularly concerning the production of hydroxyl radicals, is required prior to introduce this technique to water treatment at an industrial scale. There are two major gaps in understanding catalytic ozonation. First, is not completely clear whether catalysts cause ozone decomposition leading to the formation of hydroxyl radicals. Some recent papers used electron paramagnetic resonance to show that the presence of metal oxides accelerates the generation of hydroxyl radicals during ozonation [12]. However, there is still no direct evidence of ozone adsorption on metal oxides in the presence of water and whether the decomposition of ozone leads to the formation of surface-bound radicals or other surface oxidizing species [13]. Second, it is not known whether the adsorption of organics on the surface of catalyst plays a role in the process. Certain authors reported high adsorption of organic molecules on catalysts, but the presence of salts and other competing compounds makes it difficult to assess the importance of the adsorption of organic molecules during catalytic ozonation.

The purpose of our work was to use kinetic data to determine whether the adsorption of organic molecules results or not in an interaction between adsorbate and catalytic surface leading to an energetically favoured pathway. Besides, this study aimed to determine the influence of MnO_x on the increase of hydroxyl radicals produced from ozone and the effect of a greater surface dispersion of the oxide when using SBA as support instead of activated alumina.

2. Materials and methods

2.1. Materials

Atrazine, linuron, potassium indigotrisulfonate and sodium thiosulfate were high-purity analytical grade reagents supplied by Sigma–Aldrich. The formulation of buffers and pH adjustments were made with analytical grade reagents from Merck or Sigma–Aldrich. MiliQ ultrapure water with a resistivity of at least 18 MΩ cm at 25 °C was obtained from a Milipore system.

The heterogeneous catalysts used in this study were alumina supported manganese oxide (MnO_x/Al_2O_3) and manganese oxide supported on SBA-15. As to the former, the activated alumina was purchased from Sigma–Aldrich and used as received. It is an activated porous aluminium oxide, with a surface area of 155 m^2 g^{-1}, determined by nitrogen adsorption, and an average particle size of 100 μm. The MnO_x/Al_2O_3 catalyst was prepared by incipient wetness impregnation of the aforementioned dried Al_2O_3 using an aqueous solution of $Mn(CH_3COO)_2{\cdot}4H_2O$ (Sigma–Aldrich). The catalyst was subsequently dried in air at 423 K and calcined at 773 K for 3 h. The catalyst was washed twice in phosphate buffered water (PBW) to avoid further leaching of manganese. The amount of manganese corresponded to a 10.2 wt.% expressed as MnO_2 and

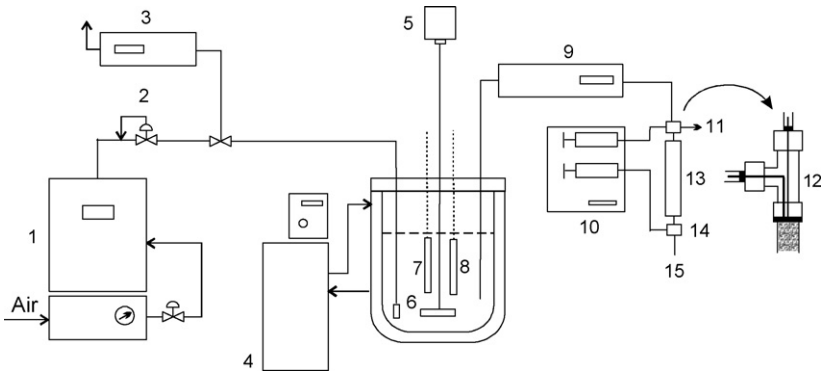

Fig. 1. Experimental equipment: (1) ozone generator; (2) flow control; (3) gas-phase UV ozone analyser; (4) thermostatic unit; (5) stirrer; (6) gas diffuser; (7) ozone amperometric sensor; (8) pH electrode; (9) HPLC pump; (10) dual-channel syringe pump; (11) sampling device; (12) detail of tubing inserts; (13) fixed-bed reactor; (14) low dead-volume mixer, (15) sampling device.

calculated by weight difference after washing and calcination. The BET surface area was 119 $m^2\,g^{-1}$ for the manganese oxide catalyst with an average pore size of 6 nm which has been calculated using the Broekhoff and de Boer (BdB) method.

MnO_x/SBA-15 was prepared by the impregnation of silica SBA-15. The method of obtaining silica SBA-15 was as follows. Pluronic P123 (Aldrich $EO_{20}PO_{70}EO_{20}$, EO: ethylene oxide, PO: propylene oxide, MW = 5800) and tetraethoxysilane (TEOS 98% GC Aldrich) were used as received. In a typical synthesis, 6 g of Pluronic P123 were stirred at 308 K in 45 g of water and 180 g of 2 M HCl solution until total dissolution. TEOS (12.5 g) was added to the solution and stirred at 308 K for 20 h. The mixture was aged at 373 K for 24 h. The white powder was recovered through filtration, washed with water and dried at 323 K overnight. The product was calcined at 773 K for 12 h with a heating rate of 1 K min^{-1}. The impregnation of the SBA-15 was carried out by the minimum volume method. In a typical impregnation the desired amount of manganese precursor, manganese nitrate tetrahydrate (Fluka) 2.01 g was dissolved in 30 mL of water and the solution poured slowly over 5 g of calcined SBA-15 while being stirred. The stirring was continuous for 10 h and the solid dried out at 323 K overnight. The catalyst was activated under calcinations at 773 K for 12 h, with heating rate of 1 K min^{-1}. The prepared catalysts presented 11.9 wt.% of MnO_2 measured after washing with PBW and calcination. MnO_x/SBA-15 had a particle size of 1.3 ± 0.2 μm as determined by DLS using a Malvern Zetasizer instrument. BET surface area was 650 $m^2\,g^{-1}$ as measured by nitrogen adsorption. We obtained a narrow pore size distribution around 5 nm using the BdB method.

The IEP of catalysts was obtained by measuring the ζ-potential in aqueous solutions at 25 °C and at various pH values after adjusting ionic strength to 10^{-3} M with NaCl. The value of IEP for MnO_x/Al_2O_3 as prepared was 7.3, which fell to 3.0 after contact with bubbling ozone in aqueous slurry for 30 min. For MnO_x/SBA-15 ζ-potential was low at working conditions, with a value of -1.3 ± 0.8 mV at pH 6.5 indicating an almost neutral surface that became negatively charged after contact with bubbling ozone. The decrease of ζ-potential during ozonation could be attributed to the production of negatively-charged surface oxygen-containing groups [11], but it is also relevant for the possible adsorption of organics through ion-exchange.

2.2. Ozonation procedure

The runs were performed using ozone stock solution stored in a tank kept at 25 °C in which ozone was continuously bubbled using a diffuser. The stock was kept at pH 6.5 using 0.1 M PBW. The reason for using phosphate buffer was to ensure a constant pH inside the reactor where external adjustments are not possible. pH in the feed tank was continuously monitored by means of a Eutech alpha-pH100 feed-back control device. The concentration of ozone in the stock tank varied in the 5.0–10.0 mg/L range according to the prescribed dose for each run. The ozone solution was delivered to the reactor at a flow-rate of 2.0–4.5 mL/min using a HPLC Shimadzu pump. The experiments were conducted using stock solutions of 4.5 mg/L of atrazine (20.9 mM) and 5.0 mg/L of linuron (20.1 mM) at a flow-rate of 0.6–1.6 mL/min, which represented a maximum dilution factor of 7.5 in the PBW charged with ozone. The solution containing organics was delivered using a Harvard Dual Syringe Pump, which also pumped the quenching agent that stopped reaction. In preliminary runs, we monitored the temperature and the inlet, outlet and inside the bed with no significant deviations (±1.5 °C) from the stock temperature of 25 °C. The tee located at the reactor head was provided with two PVDF internal tubes in order to avoid the mixing of ozone charged water with the solution containing the organic reagent before reaching the catalytic bed. Details on the experimental set-up are given in Fig. 1.

All reactions were performed with an excess of ozone. The residual oxidant in the exit mixture was quenched with the indigo reagent so that the reaction immediately stopped and the concentration of ozone could be determined. As an alternative, sodium thiosulfate was used for ozone quenching to ensure the absence of interferences in HPLC measurements. The length of the columns filled with catalyst was either 90 or 50 mm with an inside diameter or 4.6 mm. Both MnO_x/Al_2O_3 and MnO_x/SBA-15 were diluted with Al_2O_3 and SBA-15 of the same granulometry at 2.5% and 10%, leading to 0.25% and 1.0% of MnO_2 with respect to the whole bed. For higher loads, and due to the low liquid-to-catalyst ratio used in this work, no residual ozone could be observed in the exit stream. In all cases, after establishing the desired flow-rates, the concentration of ozone at the reactor inlet was determined using a sample valve as indicated below. All runs using the same concentration of catalyst were performed with the same column, which had been preconditioned with ozone for at least 2 h before performing the first measurement. By periodically checking with reference conditions, no loss of efficiency or deactivation could be measured for any of the catalytic beds used in this work during their service period. Additional bath runs were performed to determine the rate constants for direct ozonation in the presence of t-BuOH following a procedure described elsewhere [7].

2.3. Analyses

The concentration of ozone dissolved in the aqueous phase was monitored with an amperometric Rosemount 499AOZ analyzer periodically calibrated using the Indigo Colorimetric Method (SM

4500-O3 B). The same colorimetric method was used to determine the ozone at the reactor inlet and outlet. The analyses of atrazine and linuron were performed by HPLC using a Hewlett Packard 1200 Series device (Agilent Technologies, Palo Alto, USA) equipped with a reversed phase Kromasil 5u 100A C18 analytical column. The mobile phase was a mixture of acetonitrile (60%) and water (40%). UV detection was carried out at 210 nm (linuron) and 228 nm (atrazine). Nitrogen adsorption isotherms were measured at 77 K using a Beckman-Coulter SA3100 system on samples that were previously outgassed overnight at 200 °C.

3. Results and discussion

It is well known that the presence of particles smoothes out the laminar velocity profile and results in a uniform profile provided that the wall effects and axial dispersion are negligible. The effect of higher bed porosity in the vicinity of the reactor wall can be neglected if the ratio of the reactor diameter to the particle diameter is larger than 10. Similarly, the axial dispersion can be neglected using a ratio of reactor length to particle diameter of over 50 [14]. In this work and for the most unfavourable case the aforementioned ratios were 44 and 480 respectively. Bed porosity was estimated in line with Haughey and Beveridge [15].

Prior to ozonation runs, the adsorption of atrazine and linuron was assessed in batch runs. After 24 h in contact with any of the catalysts used in this work, the amount adsorbed was below statistical significance in PBW. In a previous work we obtained similar results for fenofibric acid on MnO_x/Al_2O_3 both in PBW and wastewater [7]. Other studies have reported the lack of significant adsorption of organics on various catalysts including supported manganese oxide at several pH values, a result which may suggest that the reaction probably occurs mainly in the aqueous phase and not on the catalyst surface [16].

The rate of depletion of a given organic compound in an ozonation process is the consequence of its second order parallel reaction with dissolved ozone and with hydroxyl radicals as indicated in Eq. (1). According to Elovitz and von Gunten's hypothesis, the ozonation process is characterized by R_{ct}, the ratio of the concentration of hydroxyl radicals and ozone, that represents the efficiency of the system in generating hydroxyl radicals [17].

$$r_A^h(\text{mol L}^{-1}\,\text{s}^{-1}) = k^h_{O_3} c_A c_{O_3} + k^h_{HO\bullet} c_A c_{HO\bullet} = (k^h_{O_3} + k^h_{HO\bullet} R^h_{ct}) c_A c_{O_3} \quad (1)$$

The preceding equation has been written in homogeneous units; a superscript "*h*" indicating homogeneous reaction. In what follows we assumed an average value for the ratios R_{ct} and R^c, the last defined below. Although both parameters may change during an ozonation reaction, the conversion of atrazine and linuron was in all cases low enough to accept that these values could be representative of the first part of the ozonation, where there is still a considerable amount of the parent compounds in solution. Additional details on this point are given elsewhere [7]. In the presence of a solid catalyst, the rate of ozonation is also the result of parallel direct and hydroxyl-mediated oxidation on the catalyst surface in a reaction that may involve adsorbed species. Assuming adsorption equilibrium and low surface coverage, the rate expression becomes linear with the concentration of organic adsorbate [18]. The interaction of ozone and catalytic surface has been shown to increase the amount of surface hydroxyl groups that have been recognized as the active sites for ozone decomposition on transition metal oxides [19]. As a consequence of this interaction, ozone-adsorbed species S-OH$(O_3)_s$ or the product of the evolution of hydroxyl radicals or oxygen, S–$O_3^\bullet$ or S–$O^\bullet$ respectively, where "S" refers to surface of the catalyst [16]. The primary formation of oxidized surface sites in then due to the following reaction:

$$O_3 + S - OH \overset{K}{\rightleftarrows} S - OH(O_3)_s \quad (2)$$

Considering this equilibrium, and c_s being the concentration of surface sites available for ozone binding, is, the concentration of dissolved ozone determines the amount of oxidized surface sites [20]:

$$c_{(O_3)_s} = K c_{O_3} c_s = \frac{K c_{O_3} c_t}{1 + K c_{O_3}} \quad (3)$$

where c_t is the total concentration of surface sites and it was assumed that the adsorption of organics do not interfere with the interaction of the surface with ozone. For $Kc_{O_3} >> 1$, Eq. (3) reverts to an expression similar to the definition of R_{ct} in homogeneous systems in which we considered that the concentration of dissolved ozone at the catalyst surface equals the ozone concentration in the bulk due to its low reaction rate:

$$c_{(O_3)_s} = R^c c_{O_3} \quad (4)$$

Without loss of generality, $c_{(O_3)_s}$ may be substituted by the concentration of oxidized surface, c_{ox}, sites yielding the following overall rate constant expression for a catalytic process:

$$r^c\left(\text{mol kg}^{-1}\,\text{s}^{-1}\right) = k^c_{O_3} c_A c_{O_3} + k^c_{ox} c_A c_{ox} = k^c_{O_3} c_A c_{O_3} + k^c_{ox} R^c c_A c_{O_3} = \left(k^c_{O_3} + k^c_{ox} R^c\right) c_A c_{O_3} \quad (5)$$

where the superscript "*c*" stands for catalytic reactions. This equation is valid either for the interaction with an organic molecule in the liquid phase by an Eley–Rideal mechanism or for the reaction between adsorbed species provided the adsorption equilibrium constant is low [18]. The rate of ozonation can be obtained combining Eqs. (1) and (5) and expressed in heterogeneous units are as follows:

$$r_A = \left(\frac{\varepsilon}{\rho_b} k^h_{O_3} + k^c_{O_3}\right) c_A c_{O_3} + \left(\frac{\varepsilon}{\rho_b} k^h_{HO\bullet} c_{HO\bullet} + k^c_{ox} c_{ox}\right) c_A = \left(\frac{\varepsilon}{\rho_b} k^h_{O_3} + k^c_{O_3} + \frac{\varepsilon}{\rho_b} k^h_{HO\bullet} R^h_{ct} + k^c_{ox} R^c\right) c_A c_{O_3} = k_1 c_A c_{O_3} \quad (6)$$

where ε and ρ_b are bed porosity and bulk density respectively. The decomposition of ozone also takes place following parallel catalytic and homogeneous processes.

$$r_{O_3}(\text{mol kg}^{-1}\,\text{s}^{-1}) = \frac{\varepsilon}{\rho_b} r^h_{O_3} + r^c_{O_3} = \frac{\nu\varepsilon}{\rho_b} k^h_{O_3} c_A c_{O_3} + \nu k^c_{O_3} c_A c_{O_3} + \frac{\varepsilon}{\rho_b} k^h_d c_{O_3} + k^c_d c_{O_3} = \nu\left(\frac{\varepsilon}{\rho_b} k^h_{O_3} + k^c_{O_3}\right) c_A c_{O_3} + \left(\frac{\varepsilon}{\rho_b} k^h_d + k^c_d\right) c_{O_3} = k_2 c_A c_{O_3} + k_3 c_{O_3} \quad (7)$$

where ν is the stoichiometric coefficient for the direct reaction between the organic compound and ozone. The mass balance to a differential reactor volume yields the following equations:

$$\frac{dW}{F_o} = -\frac{dc_A}{r_A} \quad (8)$$

$$\frac{dW}{F_o} = -\frac{dc_{O_3}}{r_{O_3}} \quad (9)$$

The combination of the integrated forms of the preceding equations with the expanded forms of r_A and r_{O_3} allows the experimental determination of the constants k_1, k_2 and k_3, which represent a combination of the fundamental kinetic parameters governing the ozonation process, as explained below. The mass balance to a differential reactor volume can also be expressed as follows:

$$\frac{dc_A}{dc_{O_3}} = \frac{r_A}{r_{O_3}} = \frac{k_1 c_A c_{O_3}}{k_2 c_A c_{O_3} + k_3 c_{O_3}} \quad (10)$$

If there are more than one organic oxidizable compound, a similar equation can be written for both, which is the basis of the competitive method of kinetic analysis

$$\frac{dc_A}{dc_B} = \frac{r_A}{r_B} \quad (11)$$

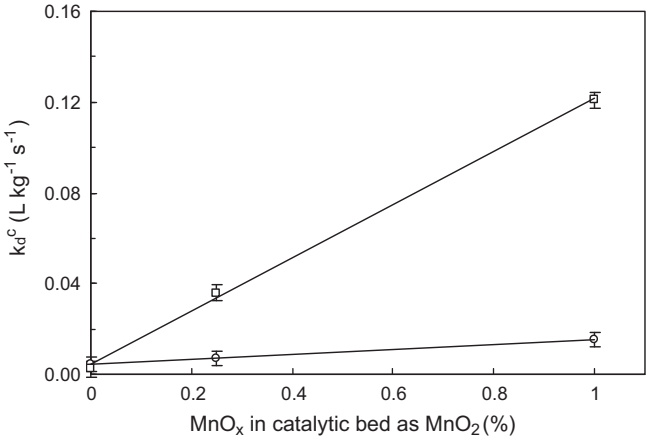

Fig. 2. Rate constant for the catalytic decomposition of ozone on MnO_x/Al_2O_3 (○) and MnO_x/SBA-15 (□) as a function of the content of manganese oxide in the catalytic bed calculated as MnO_2.

In a first series of runs, we determined the rate of catalytic decomposition of ozone in the absence of organic compounds. The rate constant for the homogeneous decomposition of ozone in PBW was determined in semicontinuous experiments using PBW previously loaded with ozone and following a procedure described elsewhere [21]. The value obtained was $k_d^h = (2.10 \pm 0.45) \times 10^{-3}\ s^{-1}$. The value of k_d^c, derived from Eq. (7), was $0.0044 \pm 0.00020\ L\,kg^{-1}\,s^{-1}$ for Al_2O_3 and $0.0023 \pm 0.0031\ L\,kg^{-1}\,s^{-1}$ for SBA-15, where the boundaries represent 95% confidence intervals, the last not differing significantly from zero. The incorporation of manganese forming MnO_x/Al_2O_3 or MnO_x/SBA-15 resulted in a considerable increase in the catalytic rate of ozone decomposition as shown in Fig. 2. With 10% MnO_x/SBA-15 (1.0 wt.%. of bed as MnO_2), the kinetic constant increased up to $0.123 \pm 0.004\ L\,kg^{-1}\,s^{-1}$. Expressed in pseudo-homogeneous units (s^{-1}) this amounts a 30 fold increase with respect to the constant for non-catalytic ozone decomposition. The corresponding kinetic constant for MnO_x/Al_2O_3 loaded with 10% MnO_2 (1.0 wt.%. of bed as MnO_2) was $0.0155 \pm 0.0015\ L\,kg^{-1}\,s^{-1}$. The relative efficiency for ozone decomposition of MnO_x/SBA-15 and MnO_x/Al_2O_3 is somewhat larger than that expected from their respective surface areas. This may reflect a better dispersion of MnO_x on silica, probably as a consequence of the differences in the metal oxide–support interaction. Moreover, the uniform pore-size distribution in the ordered mesoporous materials could allow for a better particle size control of the active phase.

During the ozonation of a given organic compound, Eq. (10) can be integrated along the reactor to yield the following expression:

$$\frac{k_2}{k_1}(c_{Ao} - c_{As}) + \frac{k_3}{k_1}\ln\left(\frac{c_{Ao}}{c_{As}}\right) = \left(c_{O_3 o} - c_{O_3 s}\right) \tag{12}$$

Using experimental values for the concentrations of organic compound and ozone from runs performed at different spatial velocities, a regression analysis yields values for k_2/k_1 and k_3/k_1. The ratio k_2/k_1 can be rearranged from Eqs. (6) and (7) as follows:

$$\frac{k_2}{k_1} = \frac{(\nu\varepsilon/\rho_b)k_{O_3}^h + \nu k_{O_3}^c}{(\varepsilon/\rho_b)k_{O_3}^h + k_{O_3}^c + (\varepsilon/\rho_b)k_{HO\bullet}^h R_{ct}^h + k_{ox}^c R^c} \tag{13}$$

The compounds tested in this work have a low value of $k_{O_3}^h$ that is $6\ M^{-1}\,s^{-1}$ for atrazine [22], and $1.9\ M^{-1}\,s^{-1}$ for linuron [23]. Batch runs performed in the presence of t-BuOH 10 mM, a well-known radical scavenger, allowed the calculation of the direct catalytic rate constants for degradation of atrazine and linuron, $k_{O_3}^c$. We found no evidence that these values were significantly different from zero, the conversion of both compounds being completely explained by the homogeneous direct ozonation reaction. This result agrees with the negligible extent of adsorption observed for both compounds, as indicated before, and is also consistent with a low interaction between surface and neutral organics. Using these results, Eq. (13) transforms as follows:

$$\frac{k_2}{k_1} = \frac{(\nu\varepsilon/\rho_b)k_{O_3}^h + \nu k_{O_3}^c}{(\varepsilon/\rho_b)R_{ct}^h\left(k_{HO\bullet}^h + k_{ox}^c(R^c/R_{ct}^h)(\rho_b/\varepsilon)\right)} = \frac{(\nu\varepsilon/\rho_b)k_{O_3}^h + \nu k_{O_3}^c}{(\varepsilon/\rho_b)R_{ct}^h k_{HO\bullet}^{hc}} \tag{14}$$

where $k_{HO\bullet}^{hc}$ represents the apparent kinetic constant for the reaction with hydroxyl radicals in the presence of catalyst expressed in heterogeneous units. It is not a true kinetic constant, as depends on the efficiency of the system in producing homogeneous hydroxyl radicals and oxidized surface sites, but it can be readily computed and compared with the homogeneous constant $k_{HO\bullet}^h$. The same rearrangements for k_3/k_1 lead to the following expression:

$$\frac{k_3}{k_1} = \frac{(\varepsilon/\rho_b)k_d^h + k_d^c}{(\varepsilon/\rho_b)R_{ct}^h k_{HO\bullet}^{hc}} \tag{15}$$

In all cases and under the conditions tested in this work, with atrazine or linuron as organic compounds, Eq. (12) yielded experimental values for k_2/k_1 that did not differ significantly from zero. This is clearly due to the low value of the direct ozonations constants for both compounds. The value of k_3 can be obtained from the experimental data for ozone concentration the same runs by combining and integrating Eqs. (7) and (9). As a result, k_1 can be derived from Eq. (15) and, from it, the experimental values of $k_{HO\bullet}^{hc}R_{ct}^h$ have been computed. The effect of catalyst could result in an enhancement of the rate of hydroxyl radical production from ozone, R_{ct}^h, an increase in the catalytic rate constant between organics and hydroxyl radicals, included in $k_{HO\bullet}^{hc}$, or both. In order to gain further insight on this point, we performed a series of simultaneous ozonation runs of atrazine and linuron in PBW and in the presence of bicarbonate 10^{-3} M and 5×10^{-3} M. The competitive kinetic method applied to a differential section of the fixed bed yields:

$$\frac{dc_A}{dc_B} = \frac{r_A}{r_B} = \frac{k_{1,A}c_A c_{O_3}}{k_{1,B}c_B c_{O_3}} = \frac{c_A k_{HO\bullet,A}^{hc}}{c_B k_{HO\bullet,B}^{hc}} \tag{16}$$

And integrating between inlet and outlet compositions:

$$\ln\left(\frac{c_{A.o}}{c_{A,s}}\right) = \frac{k_{HO\bullet,A}^{hc}}{k_{HO\bullet,B}^{hc}}\ln\left(\frac{c_{B.o}}{c_{B,s}}\right) \tag{17}$$

In order to derive Eqs. (16) and (17), $k_{O_3}^h$ was considered as being low for both atrazine and linuron, as indicated earlier. Fig. 3 shows the results of six series of runs performed with mixtures of atrazine (A) and linuron (B) using different amounts of bicarbonate, a well-known radical scavenger that should affect R_{ct} but not $k_{HO\bullet}$. The ratio of the logarithmic concentration decays of atrazine and linuron across the catalytic bed yielded a value for $k_{HO\bullet(A)}^{hc}/k_{HO\bullet(B)}^{hc}$ of 0.49 ± 0.05, a value that is not significantly different from the ratio determined using the homogeneous second order rate constants published elsewhere and obtained at 20 °C, namely, $k_{HO\bullet(A)}^{hc}/k_{HO\bullet(B)}^{hc} = 0.43 \pm 0.04$ [22–24]. This result offers no evidence that any of the catalysts may contribute to an increase in the second order rate constant for the reaction between organics and hydroxyl radicals. To be more precise, the experimental results shows no evidence that $k_{ox}^c(R^c/R_{ct}^h)(\rho_b/\varepsilon)$ is significantly different from zero. If the catalytic reaction with hydroxyl radicals involved adsorbed organics, it might be expected that the rate constant $k_{HO\bullet}^{hc}$, due to the effect of k_{ox}^c, would differ from that of the homogeneous system, $k_{HO\bullet}^h$ and that this difference would also affect their ratio. There is the possibility that the rate constant could increase both for atrazine and

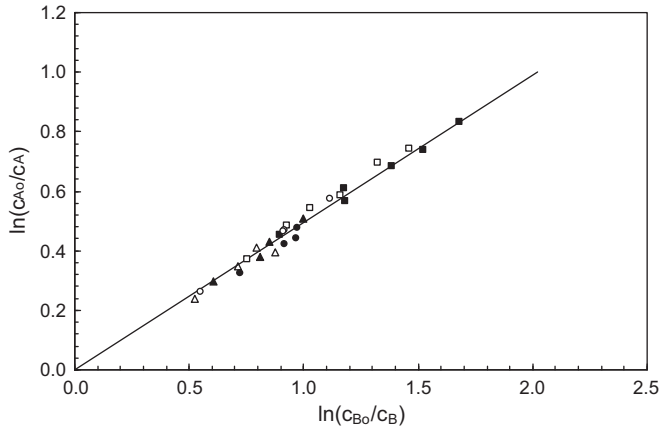

Fig. 3. Logarithmic decay of concentrations of atrazine (A) and linuron (B) in ozonation runs of mixtures of both compounds using MnO_x/Al_2O_3 (□) and MnO_x/SBA-15 (■) in PBW and MnO_x/Al_2O_3 10^{-3} M $NaHCO_3$ (○), MnO_x/Al_2O_3 5×10^{-3} M $NaHCO_3$ (△), MnO_x/SBA-15 10^{-3} M $NaHCO_3$ (●) and MnO_x/SBA-15 5×10^{-3} M $NaHCO_3$ (▲). (1.0 wt.% of MnO_2 in all beds.).

linuron cancelling the effect on the ratio of rate constants, but our previous findings pointed to a low degree of interaction between surface and organics if any. For it, the ozonation of fenofibric acid in several matrixes had already demonstrated that neither Al_2O_3 nor MnO_x/Al_2O_3 had any observable effect on its indirect ozonation rate constant even when hydroxyl radical-to-ozone ratio was significantly improved by both catalysts [7].

In what follows, we used the result that $k^{hc}_{HO\bullet}$ did not differ from their corresponding homogeneous values, $k^{h}_{HO\bullet}$ for atrazine and linuron in order to derive average values for R^h_{ct} from the experimental values of k_3/k_1 using Eq. (15). It must be noted that the conclusion concerning the lack of interaction of atrazine and linuron with the catalytic surface is not dependent on the particular values of R^h_{ct} or R^c. Fig. 4 plots the average hydroxyl radical-to-ozone ratio within the reactor for ozonation runs of atrazine as a function of the moles of ozone consumed per mole of atrazine. The values were obtained in several reactors containing Al_2O_3, SBA-15 and two different amounts of MnO_x loaded on both supports. The plot shows that R^h_{ct} decreased with the moles of ozone consumed, whose higher values also corresponded to higher atrazine conversions. This behaviour may be a consequence of the disappearance from solution of the parent aromatic compounds. In fact, it has been stated that the decomposition of ozone and the production of hydroxyl radicals are strongly promoted by aromatic solutes due to the formation of hydrogen peroxide as an intermediate product [25]. Other compounds such as oxoacetic acids, typically found as ozonation by-products, contribute to ozone decomposition and to the formation of radicals such as superoxide and hydroperoxyl, and may contribute to this effect [26].

Fig. 4 also shows that R^h_{ct} was considerably promoted by MnO_x/Al_2O_3 with values near or over 10^{-6} whereas the maximum value obtained for Al_2O_3 was 3.7×10^{-7} for atrazine conversions <10%. A much higher effect could be appreciated when MnO_x was incorporated into SBA-15, with R^h_{ct} as high as 3.0×10^{-6} while in similar conditions SBA-15 alone hardly surpassed 10^{-7}. This represented an average 30 fold increase in R_{ct} when using MnO_x/SBA-15 with respect to SBA-15 alone, whereas MnO_x/Al_2O_3 increased the efficiency in generation hydroxyl radicals by an average factor of 2.7 with respect to Al_2O_3. For MnO_x/SBA-15, R_{ct} increased threefold with respect to MnO_x/Al_2O_3 under similar conditions.

The use of catalyst also led to a lower ozone consumption per mole of converted organic compound as observed in Fig. 5,which gives R^h_{ct} for runs performed using mixtures of linuron and atrazine

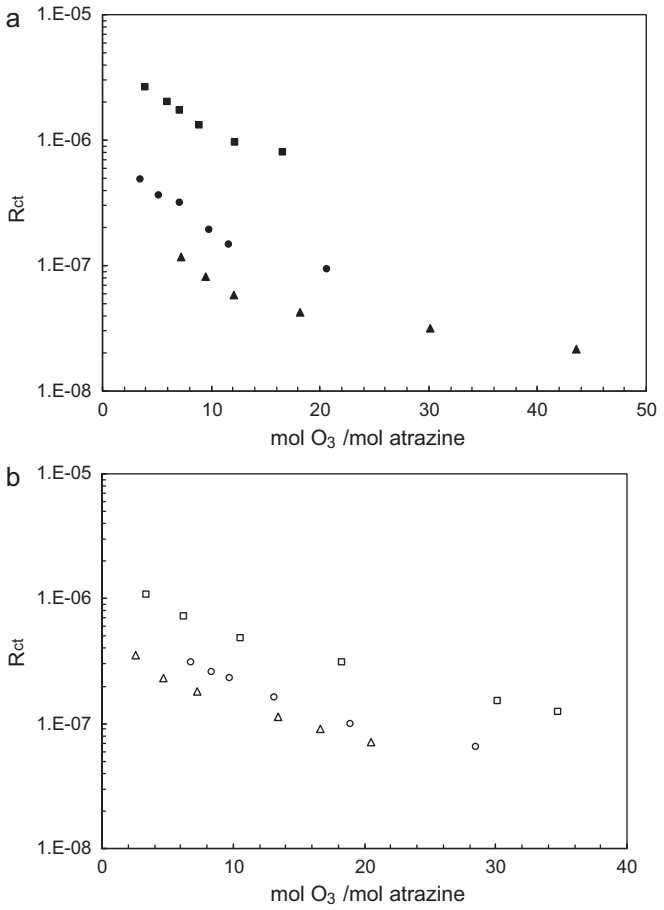

Fig. 4. Hydroxyl-radical-to-ozone ratio, R^h_{ct}, for the catalytic ozonation of atrazine on MnO_x/SBA-15 (a, filled symbols) and MnO_x/Al_2O_3 (b, empty symbols) using a MnO_2 load of 1.0 wt.% (squares), 0.25 wt.% (circles) and 0% (Al_2O_3 or SBA-15, triangles).

on MnO_x/Al_2O_3 and MnO_x/SBA-15 in PBW loaded with different concentrations of bicarbonate. The increase in R^h_{ct} was parallel to the decrease in the moles of ozone consumed and was more intense for the case of MnO_x/SBA-15 catalyst. The lower ozone consumption corresponded to runs with high space velocities and, therefore, lower conversions, typically less than 10% ozone conversions for

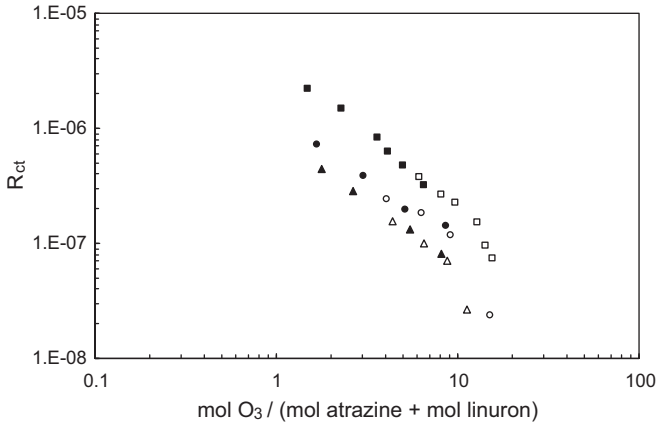

Fig. 5. Hydroxyl-radical-to-ozone ratio, R^h_{ct}, for the catalytic ozonation of mixtures of atrazine and linuron as a function of the moles of ozone consumed per mole of atrazine or linuron oxidized. MnO_x/Al_2O_3 (□) and MnO_x/SBA-15 (■) in PBW; MnO_x/Al_2O_3 10^{-3} M $NaHCO_3$ (○), MnO_x/SBA-15 10^{-3} M $NaHCO_3$ (●); MnO_x/Al_2O_3 5×10^{-3} M $NaHCO_3$ (△), and MnO_x/SBA-15 5×10^{-3} M $NaHCO_3$ (▲). (1.0 wt.% of MnO_2 in all beds.).

runs with efficiencies near 1.5 moles of ozone per mole of converted parent organic, atrazine or linuron.

4. Conclusions

A kinetic study of the catalytic ozonation of atrazine and linuron was carried out in a two-phase fixed-bed reactor operating in excess of ozone with ozone-preloaded phosphate buffered water. A catalyst with a larger specific surface, MnO_x/SBA-15, improved the rate of ozone decomposition with a kinetic constant of $0.123 \pm 0.004\,L\,kg^{-1}\,s^{-1}$ for a total metal bed load of 1.0% expressed as MnO_2. In the same conditions, the ozone decomposition rate constant was $0.0155 \pm 0.0015\,L\,kg^{-1}\,s^{-1}$ for MnO_x/Al_2O_3. The incorporation of MnO_x to SBA-15 (1.0% as MnO_2) resulted in a 30 fold increase in the rate constant with respect to the non-catalytic ozone decomposition constant in the same matrix.

Neither atrazine nor linuron adsorbed significantly on any of the catalysts in PBW. Consistent with this result, we found that the direct catalytic ozonation constant did not differ significantly from zero in any case, the reaction with molecular ozone being essentially the non-catalytic process taking place in homogeneous phase. The results of catalytic runs on both catalysts and using different concentrations of bicarbonate did not show any evidence that MnO_x/Al_2O_3 or MnO_x/SBA-15 increased the indirect, hydroxyl-mediated, ozonation rate constant with respect to homogeneous ozonation. This results suggests the absence of surface interaction with atrazine and linuron and may indicate that their adsorption did not take place at all. In any case, a possible adsorption of organics did not result in an energetically favoured route for the catalytic reaction with hydroxyl radicals.

The efficiency of hydroxyl radical production from ozone was significantly improved by the use of catalysts with average hydroxyl radical-to-ozone ratio within the reactor near 10^{-6} for MnO_x/Al_2O_3 and up to 3.0×10^{-6} for MnO_x/SBA-15. This represented a considerable - up to 30 fold - increase in the average value for R_{ct}^h with respect to the support alone for MnO_x/SBA -15. R_{ct}^h for MnO_x/SBA-15 was about three times its value for MnO_x/Al_2O_3 under similar conditions. The use of catalyst also led to lower ozone consumption per mole of converted organic compound, whether or not bicarbonate was present in the solution, the highest efficiency being obtained for MnO_x/SBA-15. The relative efficiency of MnO_x/SBA-15 with respect to MnO_x/Al_2O_3 is most probably the consequence of a better distribution of the active phase on a larger surface.

Acknowledgements

This work has been financed by Spain's Ministry of Education (CSD2006-00044) and the Dirección General de Universidades e Investigación de la Comunidad de Madrid, Research network 0505/AMB-0395.

References

[1] EC, Directive of the European parliament and of the council 2000/60/EC establishing a framework for community action in the field of water policy, Official Journal, 2000, C513, 23/10/2000.
[2] R. Andreozzi, V. Caprio, A. Insola, R. Marotta, Advanced oxidation processes (AOP) for water purification and recovery, Catal. Today 53 (1999) 51–59.
[3] P.R. Gogate, A.B. Pandit, A review of imperative technologies for wastewater treatment I: oxidation technologies at ambient conditions, Adv. Environ. Res. 8 (2004) 501–551.
[4] P.R. Gogate, A.B. Pandit, A review of imperative technologies for wastewater treatment II: hybrid methods, Adv. Environ. Res. 8 (2004) 553–597.
[5] B. Kasprzyk-Hordern, M. Ziolek, J. Nawrocki, Catalytic ozonation and methods of enhancing molecular ozone reactions in water treatment, Appl. Catal. B: Environ 46 (2003) 639–669.
[6] C.M. Jonsson, C.L. Jonsson, D.A. Sverjensky, H.J. Cleaves, R.M. Hazen, Attachment of L-glutamate to rutile (α-TiO_2): a potentiometric, adsorption, and surface complexation study, Langmuir 25 (2009) 12127–12135.
[7] R Rosal, M.S. Gonzalo, A. Rodríguez, E. García-Calvo, Catalytic ozonation of fenofibric acid over alumina-supported manganese oxide, J. Hazard. Mater. 183 (2010) 271–278.
[8] J.P. Kaptijn, The Ecoclear® process. Results from full-scale installations, Ozone Sci. Eng. 19 (1997) 297–305.
[9] S.H. Lin, C.L. Lai, Kinetic characteristics of textile wastewater ozonation in fluidized and fixed activated carbon beds, Water Res. 34 (2000) 763–772.
[10] J. Ma, M. Sui, T. Zhang, C. Guan, Effect of pH on MnO_x/GAC catalyzed ozonation for degradation of nitrobenzene, Water Res. 39 (2005) 779–786.
[11] X. Qu, J. Zhenga, Y. Zhanga, Catalytic ozonation of phenolic wastewater with activated carbon fiber in a fluid bed reactor, J. Colloid. Interface Sci. 309 (2007) 429–434.
[12] Y. Yangm, J. Ma, Q. Qin, X. Zhai, Degradation of nitrobenzene by nano-TiO_2 catalyzed ozonation, J. Mol. Catal. A: Chem. 267 (2010) 41–48.
[13] J. Nawrocki, B. Kasprzyk-Hordern, The efficiency and mechanisms of catalytic ozonation, Appl. Catal. B: Environ. 99 (2010) 27–42.
[14] Y. Schuurman, Aspects of kinetic modeling of fixed bed reactors, Catal. Today 138 (2008) 15–20.
[15] D.P. Haughey, G.S.G. Beveridge, Local voidage variation in a randomly packed bed of equal-sized spheres, Chem. Eng. Sci. 21 (1966) 905–916.
[16] L. Yang, C. Hu, Y. Nie, J. Qu, Catalytic ozonation of selected pharmaceuticals over mesoporous alumina-supported manganese oxide, Environ. Sci. Technol. 43 (2009) 2525–2529.
[17] M.S. Elovitz, U. von Gunten, Hydroxyl radical/ozone ratios during ozonation processes. I. The R_{ct} concept, Ozone Sci. Eng. 21 (1999) 239–260.
[18] A. Rodríguez, R. Rosal, J.A. Perdigón, M. Mezcua, A. Agüera, M.D. Hernando, P. Letón, A.R. Fernández-Alba, E. García-Calvo, Ozone-based technologies in water and wastewater treatment, in: D. Barceló, M. Petrovic (Eds.), The Handbook of Environmental Chemistry, vol. 5 Part S/2. Emerging Contaminants from Industrial and Municipal Waste, Springer, Berlin, 2008, pp. 127–175.
[19] L. Zhao, J. Ma, Z. Sun, H. Liu, Mechanism of heterogeneous catalytic ozonation of nitrobenzene in aqueous solution with modified ceramic honeycomb, Appl. Catal. B: Environ. 89 (2009) 326–334.
[20] F.J. Beltrán, F.J. Rivas, R. Montero, Catalytic ozonation of oxalic acid in an aqueous TiO_2 slurry reactor, Appl. Catal. B: Environ. 39 (2002) 221–231.
[21] R. Rosal, A. Rodríguez, M.S. Gonzalo, E. García-Calvo, Catalytic ozonation of naproxen and carbamazepine on titanium dioxide, Appl. Catal. B: Environ. 84 (2008) 48–57.
[22] U. von Gunten, Ozonation of drinking water. Part I. Oxidation kinetics and product formation, Water Res. 37 (2003) 1443–1467.
[23] F.J. Benítez, F.J. Real, J.L. Acero, C. Garcia, Kinetics of the transformation of phenyl–urea herbicides during ozonation of natural waters: rate constants and model predictions, Water Res. 41 (2007) 4073–4084.
[24] B. Balci, N. Oturan, R. Cherrier, M.A. Oturan, Degradation of atrazine in aqueous medium by electrocatalytically generated hydroxyl radicals. A kinetic and mechanistic study, Water Res. 43 (2009) 1924–1934.
[25] Y. Pi, J. Schumacher, M. Jekel, Decomposition of aqueous ozone in the presence of aromatic organic solutes, Water Res. 39 (2005) 83–88.
[26] J. Staehelin, J. Hoigné, Decomposition of ozone in water in the presence of organic solutes acting as promoters and inhibitors of radical chain reactions, Environ. Sci. Technol. 19 (1985) 1206–1213.